Cellular/Molecular

Modulation of NMDA Receptors by Pituitary Adenylate Cyclase Activating Peptide in CA1 Neurons Requires $G\alpha_q$, Protein Kinase C, and Activation of Src

D. S. Macdonald,[2]* M. Weerapura,[1]* M. A. Beazely,[1] L. Martin,[4] W. Czerwinski,[1] J. C. Roder,[3] B. A. Orser,[1,4] and J. F. MacDonald[1,2]

Departments of [1]Physiology, [2]Pharmacology, and [3]Immunology and [4]Institute of Medical Sciences, Faculty of Medicine, University of Toronto, Mount Sinai Hospital, Toronto, Ontario, Canada M5S 1A8

At CA1 synapses, activation of NMDA receptors (NMDARs) is required for the induction of both long-term potentiation and depression. The basal level of activity of these receptors is controlled by converging cell signals from G-protein-coupled receptors and receptor tyrosine kinases. Pituitary adenylate cyclase activating peptide (PACAP) is implicated in the regulation of synaptic plasticity because it enhances NMDAR responses by stimulating $G\alpha_s$-coupled receptors and protein kinase A (Yaka et al., 2003). However, the major hippocampal PACAP1 receptor (PAC_1R) also signals via $G\alpha_q$ subunits and protein kinase C (PKC). In CA1 neurons, we showed that PACAP38 (1 nM) enhanced synaptic NMDA, and evoked NMDAR, currents in isolated CA1 neurons via activation of the PAC_1R, $G\alpha_q$, and PKC. The signaling was blocked by intracellular applications of the Src inhibitory peptide Src(40–58). Immunoblots confirmed that PACAP38 biochemically activates Src. A $G\alpha_q$ pathway is responsible for this Src-dependent PACAP enhancement because it was attenuated in mice lacking expression of phospholipase C β1, it was blocked by preventing elevations in intracellular Ca^{2+}, and it was eliminated by inhibiting either PKC or cell adhesion kinase β [CAKβ or Pyk2 (proline rich tyrosine kinase 2)]. Peptides that mimic the binding sites for either Fyn or Src on receptor for activated C kinase-1 (RACK1) also enhanced NMDAR in CA1 neurons, but their effects were blocked by Src(40–58), implying that Src is the ultimate regulator of NMDARs. RACK1 serves as a hub for PKC, Fyn, and Src and facilitates the regulation of basal NMDAR activity in CA1 hippocampal neurons.

Key words: hippocampus; NMDA; Src; kinase; PACAP; pituitary adenylate cyclase activating peptide; signaling

Introduction

The basal level of NMDA receptor (NMDAR) activity can be considered to serve as the "set point" for the control of synaptic plasticity. The activity of these receptors is regulated by cell signals converging from a variety of G-protein-coupled receptors (GPCRs) and receptor tyrosine kinases (Kotecha and MacDonald, 2003). In schizophrenia and attention deficit hyperactivity disorder, NMDAR activity may be too low (Kotecha and MacDonald, 2003; Wong and Van Tol, 2003; Harrison and Weinberger, 2005), and some GPCRs could be therapeutic targets for enhancing NMDAR activity (Marino and Conn, 2002a,b; Conn, 2003). For example, the atypical agent clozipine may act via D_1 subtype dopamine receptor to potentiate NMDAR-mediated transmission via an Src-dependent mechanism (Wittmann et al., 2005).

The late components of long-term potentiation (LTP) in the CA1 region require the cAMP-dependent signal cascade, protein kinase A (PKA) activity, the cAMP-response element-binding protein, and alterations in protein expression (Nguyen and Woo, 2003). The pituitary adenylate cyclase activating peptide (PACAP) receptor is best known for its ability to stimulate adenylate cyclases, cAMP production, and PKA (Ohtaki et al., 1993; McCulloch et al., 2002) but also signals through $G_{q/11}$ to phospholipase C (PLC) (Spengler et al., 1993; McCulloch et al., 2002). PACAP1 receptors (PAC_1Rs), specific for PACAP, are expressed predominantly in the brain, whereas VPAC receptors, which bind both VIP and PACAP, are more common in the periphery (Hashimoto et al., 1993). PACAP ligand and the PAC_1R are found in the CA1 region of the hippocampus (Shioda et al., 1998; Skoglosa et al., 1999; Zhou et al., 2000a,b). PACAP stimulates both PKA and protein kinase C (PKC)-dependent signaling pathways (Zhou et al., 2001), suggesting a potential role for PACAP in this region of the hippocampus. Indeed, low concentrations of PACAP potentiate NMDAR-mediated responses in CA1 neurons (Yaka et al., 2003) and modulate LTP in the hippocampus (Matsuyama et al., 2003). Furthermore, transgenic mice lacking either PACAP or its major receptor (PAC_1R) display disturbances in memory retention and consolidation (Yamamoto et al., 1998; Hashimoto et al., 2002; Matsuyama et al., 2003; Shintani et al., 2004). The cellular mechanism of the acute PACAP-induced en-

hancement of NMDAR responses has been attributed to activation of the cAMP cascade (Yaka et al., 2003). In this model, Fyn is bound to receptor for activated C kinase-1 (RACK1), and PKA-dependent phosphorylation releases Fyn, allowing it to phosphorylate NMDARs (Yaka et al., 2003). This signaling by PACAP receptors contrasts with other GPCRs, which couple to $G\alpha_q$ proteins [muscarine M_1, metabotropic glutamate receptor subtype 5 (mGluR5), and lysophosphatidic acid (LPA)], to increase NMDAR activity and $EPSC_{NMDA}$s in cultured, acutely isolated and *in situ* slice hippocampal CA1 neurons (Lu et al., 1999; Huang et al., 2001; MacDonald et al., 2001; Benquet et al., 2002; Gerber, 2002; Kotecha et al., 2003; Grishin et al., 2005) via a sequential signal network composed of PLC, PKC, Ca^{2+}, cell adhesion kinase β (CAKβ), or proline-rich tyrosine kinase 2 (Pyk2)/Src. The induction of LTP at CA1 synapses also requires activation of CAKβ(Pyk2)/Src (Huang et al., 2001).

Here we show that the major PACAP ligand, PACAP38, activates PAC_1R to increase NMDA-evoked currents, and, although both $G\alpha_s$ and $G\alpha_q$ signaling pathways can be activated by PAC_1Rs, it is the $G\alpha_q$ pathway that is responsible for the enhancement of synaptic and peak NMDAR-mediated currents in CA1 neurons.

Materials and Methods

Cell isolation and whole-cell recordings. CA1 neurons were isolated from postnatal rats (Wistar, 14–22 d) or postnatal mice (28–34 d) using previously described procedures (Wang and MacDonald, 1995). To control for variation in response, recordings from control and treated cells were made on the same day. The extracellular solution consisted of the following (in mM): 140 NaCl, 1.3 $CaCl_2$, 5 KCl, 25 HEPES, 33 glucose, and 0.0005 tetrodotoxin, pH 7.4 (osmolarity between 315 and 325 mOsm). Recording electrodes with resistances of 3–5 MΩ were constructed from borosilicate glass (1.5 μm diameter; World Precision Instruments, Sarasota, FL) using a two-stage puller (PP83; Narishige, Tokyo, Japan) and filled with intracellular solution containing the following (in mM): 140 CsF, 11 EGTA, 1 $CaCl_2$, 2 $MgCl_2$, 10 HEPES, 2 tetraethylammonium, and 2 K_2ATP, pH 7.2 (osmolarity between 290 and 300 mOsm). Some drugs were included in the patch pipette. Recordings were conducted at room temperature (20–22°C). After formation of the whole-cell configuration, the neurons were voltage clamped at −60 mV and lifted into the stream of solution supplied by a computer-controlled, multi-barreled perfusion system. To monitor access resistance, a voltage step of −10 mV was made before each application of NMDA. When series resistance varied by >10%, the cell was discarded. Currents were recorded using Axopatch 1D and 200 amplifiers (Axon Instruments, Union City, CA), and data were filtered at 2 kHz and acquired using Clampex (Axon Instruments). All population data are expressed as mean ± SE. Student's *t* test was used to compare between two groups, and the ANOVA test was used to analyze multiple groups.

Recordings of miniature EPSC. Procedures for the preparation of mouse primary dissociated cultures of hippocampal neurons have been described previously (MacDonald et al., 1989). Two to 3 weeks after plating, pyramidal cells were selected for whole-cell recordings (temperature, 20–22°C). The series resistance in these recording varied between 6 and 8 MΩ, and recordings in which series resistance varied by >10% were rejected. No electronic compensation for capacitance or series resistance was applied. All solutions were the same as for isolated cells, except the extracellular solution also contained 10 μM bicuculline to inhibit GABA-mediated chloride conductance. At the holding potential of −60 mV, miniature EPSCs (mEPSCs) were recorded for 5 min both in the absence and presence of 10 μM α-amino-5-phosphonopentanoic acid (APV) before and 10 min after PACAP (1 nM) application. All mEPSCs were manually selected and averaged using Mini Analysis software (Synaptosoft, Decatur, GA). The NMDA component was obtained by subtracting the averaged mEPSC in the presence of APV from that in its absence. The amplitude of the NMDA component under control conditions and after PACAP application was compared.

Hippocampal slice preparation and recording. Hippocampal brain slices were prepared from 14- to 21-d-old Wistar rats. Briefly rats were decapitated after halothane anesthesia, and brains were quickly removed and placed in ice-cold oxygenated (95% O_2, 5% CO_2) artificial CSF (aCSF) [in mM: 124.0 NaCl, 3.0 KCl, 1.3 $MgCl_2$·$6H_2O$, 2.6 $CaCl_2$, 1.25 NaH_2PO_4·H_2O, 26 $NaHCO_3$, 10.0 D-glucose (osmolarity between 300 and 310 mOsm)]. Whole-brain coronal slices (300 μm) containing transverse sections of the hippocampus were prepared using a vibratome (VT100E; Leica, Nussloch, Germany). After a recovery period of 1 h in oxygenated aCSF, tissues were transferred to a recording chamber mounted on the stage of an upright microscope (BX51WI; Olympus Optical, Tokyo, Japan) equipped with a water immersion objective (40×; numerical aperture, 0.95; working distance, 2.0 mm), Nomarski optics, and infrared–differential interference contrast video microscopy. The CA1 region was isolated from CA3 with a surgical cut, and slices were continually perfused with 0 Mg^{2+} oxygenated aCSF (2–3 ml/min) at room temperature (22–24°C). Tight seals (>1 GΩ) were formed on the cell body of visually identified CA1 pyramidal neurons, and whole-cell voltage-clamp recordings were obtained by rupturing the membrane with negative pressure. Recording electrodes as described previously were filled with an internal solution containing the following (in mM): 140 Cs-gluconate, 11 EGTA, 10 HEPES, and 2 $MgCl_2$, pH 7.2–7.3. Cells were held at −60 mV, and series resistance was monitored throughout the recording period. Only recordings with stable holding current and series resistance maintained below 30 MΩ were considered for analysis. Schaffer collateral synapses were stimulated every 30 s with constant current pulses (50–100 μs) delivered through a concentric bipolar platinum stimulating electrode (25 μm exposed tip) positioned at the border of stratum radiatum–stratum lacunosum. Evoked $EPSC_{NMDA}$s were isolated by the addition of CNQX (20 μM) and bicuculline (10 μM). Electrode placement and intensity were contingent on evoking the largest NMDA response without eliciting an action potential or spiking artifact. PACAP was applied after 5 min of a stable baseline period, and EPSCs were recorded for the subsequent 15 min. Excitatory synaptic currents were recorded using a Multiclamp 700A amplifier (Axon Instruments), low-pass filtered at 2 kHz, and digitized at 10–20 kHz with Clamplex (version 9.2; Axon Instruments).

Membrane adenylyl cyclase assay. Hippocampal tissue from wild-type or PLCβ1-null mice was Dounce homogenized on ice in 1 ml of ice-cold buffer (15 mM HEPES, pH 7.4, 5 mM $MgCl_2$, 2 mM EDTA, 1 mM 3-isobutyl-1-methylxanthine, and 0.01% ascorbic acid). Approximately 40 μg of tissue homogenate was incubated with drugs and reaction mixture (2 mM ATP, 5 μM GTP, 20 mM phosphocreatine, and 5 U of creatine phospho-kinase) at 30°C for 15 min. The reaction was terminated by the addition of 100 μl of ice-cold 4% trichloroacetic acid. cAMP levels were determined using the BTI cAMP radioimmunoassay system (Biomedical Technologies, Stoughton, MA) according to the instructions of the manufacturer. Briefly, samples were incubated overnight with a known amount of ^{125}I 2′-0-succinyl-cAMP and a cAMP binding antibody. After incubation, samples were mixed with 1 ml of ice-cold buffer (50 mM sodium acetate and 0.01% sodium azide, pH 7.4) and centrifuged at 2000 × g for 20 min. The supernatant was decanted, and the radioactivity level bound to the antibody was determined.

Tyrosine phosphorylation of Src. The CA1 region from acute hippocampal slices from Wistar rats (14–21 d) was microdissected and allowed to recover for 2 h at room temperature (20–22°C). The CA1 region of multiple animals was pooled to provide sufficient tissue for the assay. Twenty minutes before stimulation with agonist, the tissue was transferred to extracellular fluid that containing sodium vanadate (10 μM), treated at room temperature, and then immediately frozen on dry ice. Tissue was then homogenized in ice-cold lysis buffer containing 50 mM Tris-HCl, pH 8.0, 150 mM NaCl, 2 mM EDTA, 0.1% SDS, 1% NP-40, 1 mM sodium orthovanadate, and the protease inhibitors pepstatin A (20 μg/ml), leupeptin (20 μg/ml), and sprotinin (20 μg/ml). Insoluble material was removed by centrifugation at 14,000 × g for 10 min at 4°C. The protein content of soluble material was determined by Bio-Rad (Hercules, CA) Dc protein assay. Soluble proteins (1000 μg) were incubated overnight with 8 μl of anti-Src GD 11 (Upstate Biotechnology, Lake Placid, NY). Immune complexes were isolated by the addition of 20 μl of

protein A Sepharose beads, followed by incubation for 1 h at 4°C. Immunoprecipitates were washed four times with lysis buffer. Samples were subjected to SDS-PAGE using a 10% gel transferred to a nitrocellulose membrane. Membranes were immunoblotted with monoclonal antibodies to phosphorylated tyrosine, 4G10 (1:1000 dilution; Upstate Biotechnology), or Src tyrosine 416 (provided by Dr. M. W. Salter, Hospital for Sick Children, Toronto, Ontario, Canada) or Src tyrosine 457. Membranes were then stripped and probed for total Src using anti-Src. Signals were detected with enhanced chemiluminescence (Amersham Biosciences, Arlington Heights, IL) and developed on x-ray film. Band intensity on x-ray film was quantified. For phospho-Src, the intensity of the phosphorylated signal was divided by that of total Src to control for small differences in gel loading. Experimental and control conditions were then compared and expressed as percentage of control.

Animals. All animal experimentation was conducted in accordance with the Policies on the Use of Animals at the University of Toronto. PLCβ1 wild-type and knock-out animals were provided by Dr. John Roder (Mount Sinai Hospital, Toronto, Ontario, Canada).

Drugs and peptides. The source of drugs for this study are as follows: NMDA and glycine (Sigma, St. Louis, MO), PACAP38, bisindolylmaleimide I (bis), BAPTA (Calbiochem, La Jolla, CA), PACAP(6–38) (Phoenix Pharmaceuticals, Mountain View, CA), and Src(p60^{c-Src}) (Upstate Biotechnology). CAKβ, CAKβ 457A, and Src(40–58) were provided by Dr. M. W. Salter. Peptides were synthesized by the Advanced Protein Technology Centre (Toronto, Ontario, Canada) with the following sequences: R1 (SRDKTIIMWKLTRD, RACK1 amino acids 35–48) and R6 (DLNEGKHLpYTL-DGGDIINALCFSPNRpYWR, RACK1 amino acids 220–248).

Results

Initially, the ability of low concentrations of PACAP38 (1 nM) to modulate EPSC$_{NMDA}$s at CA1 synapses was studied. Pyramidal neurons were patch clamped in a whole-cell configuration and held at −60 mV. Schaffer collateral fibers were stimulated every 30 s with constant current pulses (50–100 μs) to evoke EPSC$_{NMDA}$s. Applications of PACAP38 to these slices caused an increase in the peak amplitude of NMDA synaptic currents (Fig. 1). This enhancement reached a plateau that was 167 ± 10% (n = 6) above baseline values. We had previously observed a similar potentiation of NMDA-evoked peak currents in isolated CA1 neurons after activation of several Gα$_q$ signaling pathways, including the mGluR5, the M$_1$ muscarinic, and LPA receptors. These receptors enhance NMDARs via a sequential Gα$_q$–PLCβ–PKC–CAKβ(Pyk2)/Src signal cascade (Lu et al., 1999; Kotecha et al., 2003), and we hypothesized that PAC$_1$Rs might also activate this cascade. The final downstream enzyme in this cascade is Src. Therefore, we recorded EPSC$_{NMDA}$s using patch electrodes containing the Src inhibitory peptide Src(40–58) (25 μg/ml). This Src-specific inhibitory peptide mimics the unique domain of Src but not Fyn. Src(40–58) eliminated the PACAP38-induced potentiation of these synaptic currents, illustrating that PACAP38 causes a change in NMDA synaptic activity that is mediated by Src and not by Fyn.

To further elucidate the signaling pathway responsible for this effect, we acutely isolated individual CA1 pyramidal cells from the slices. Slice recordings are restricted in that drugs applied to the slice must permeate the tissue to exert a response at the recorded cell. Variation between slices in the depth of the recorded cell could alter the effective drug concentration at the cell. Use of acutely isolated cells avoids this restriction. In addition, isolated neurons permit a rapid application of agonist, allowing for the resolution of both peak and steady-state NMDAR currents. Furthermore, we have shown that peak currents and EPSC$_{NMDA}$s are modulated in parallel by a variety of GPCRs and growth factor receptor (Kotecha and MacDonald, 2003).
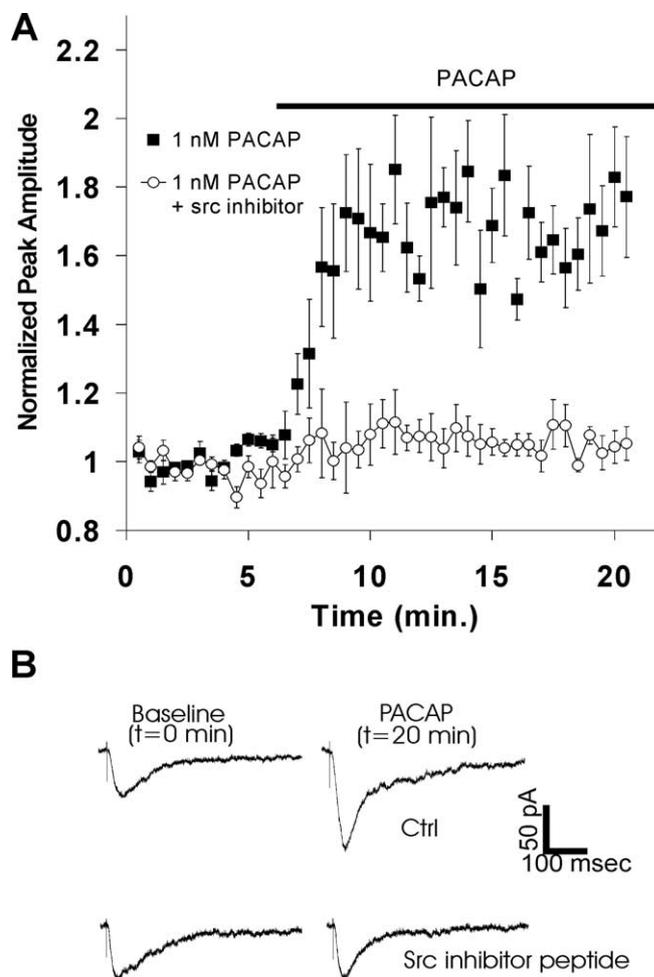
Figure 1. PACAP38 enhances NMDA currents in hippocampal slice. *A*, Application of 1 nM PACAP38 to hippocampal slices caused increased amplitude in NMDA currents. Pyramidal cells were recorded in a whole-cell configuration. NMDA peak currents reached a maximal increase ~8 min after application. Normalized peak amplitude for PACAP-treated cells was 167 ± 10% compared with baseline (n = 6). When Src(40–58) (25 μg/ml) was included in the patch pipette, PACAP38 failed to elicit a response [normalized peak current, 102 ± 2% (n = 6); p < 0.005, unpaired t test; data obtained at 20 min of recording]. The black bar indicates time and duration of 1 nM PACAP38 application. *B*, Sample traces from individual cells with and without Src(40–58) in the patch pipette at baseline (t = 0 min) and after PACAP38 application (t = 20 min).

To examine the effects of PACAP38 on NMDAR-mediated currents, PACAP38 was applied to isolated CA1 hippocampal neurons continuously for 5 min. NMDA currents were evoked once every 60 s using a 3 s exposure to NMDA (50 μM) and glycine (0.5 μM). Applications of PACAP38 (1 nM) produced a rapid and robust increase in NMDA-evoked currents (Fig. 2A). This effect outlasted the application period of PACAP38 and reached a plateau ~10 min after PACAP38 application. The increase in normalized peak currents after 20 min after PACAP application was 140 ± 5% (n = 9) compared with baseline (100%). NMDA-evoked currents were stable over the recording period, with control cells having normalized peak currents 98 ± 7% (n = 9) of baseline (Fig. 2A). The effect of PACAP38 could be seen most clearly in the peak of the NMDA-evoked current (Fig. 2B). No significant changes were seen in time constants (τ) for activation, desensitization, or inactivation phases of the recording before, during, or after PACAP38 application (data not shown). PACAP38 has been reported previously to induce enhancement of field excitatory synaptic potentials with low con-
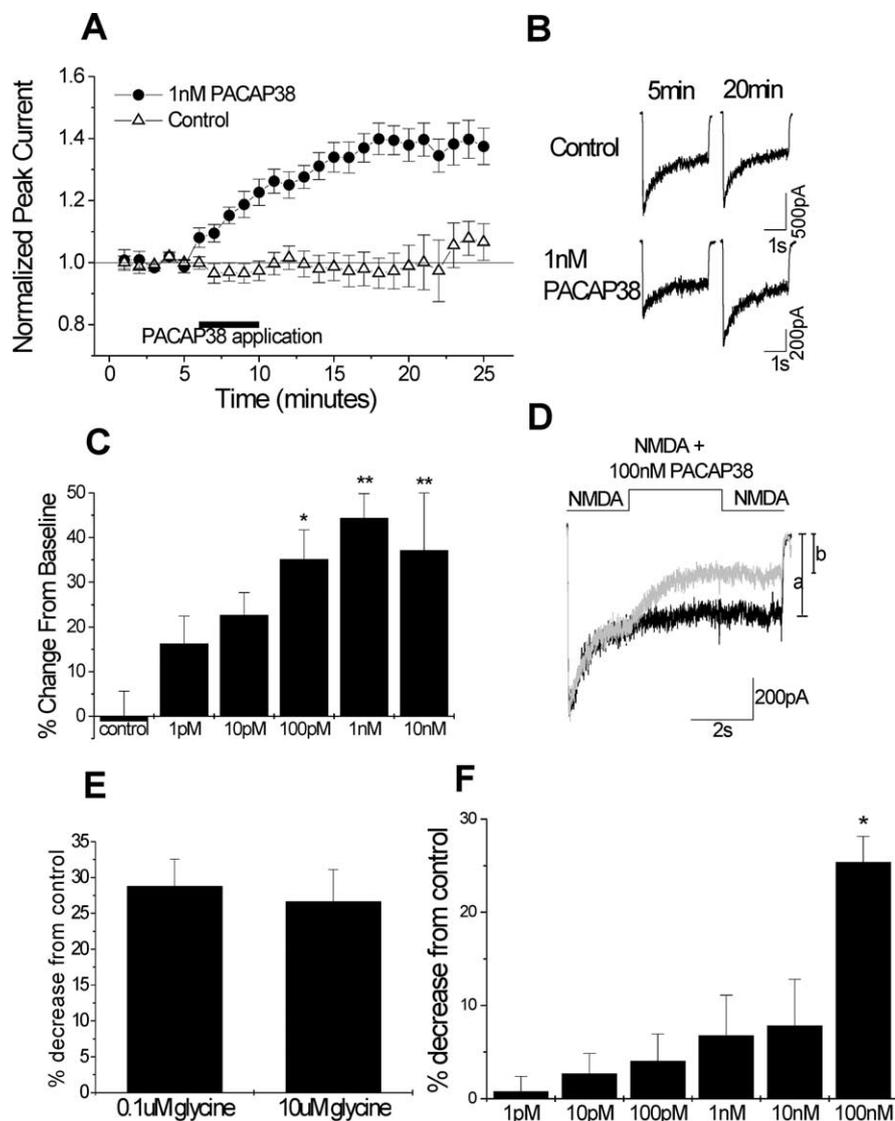
Figure 2. PACAP38 enhances peak currents in isolated CA1 pyramidal neurons. *A*, Application of PACAP38 (1 nM) to acutely isolated CA1 pyramidal neurons resulted in an increase of NMDA-evoked peak currents that outlasted the period of application, did not reverse during washout, and persisted throughout the recording period. NMDA-evoked peak currents in control cells were unchanged throughout the time course of the experiment. Cells treated with 1 nM PACAP38 had significantly larger NMDA-evoked peak currents (control, $98 \pm 7\%$, $n = 9$; 1 nM PACAP38, $140 \pm 5\%$, $n = 9$; $p < 0.001$, unpaired t test; data obtained at 20 min of recording). The black bar indicates time and duration of 1 nM PACAP38 application. *B*, Sample traces of NMDA-evoked currents for control and PACAP38-treated cells. Traces represent points immediately before PACAP38 application ($t = 5$ min) and 10 min after PACAP38 application ($t = 20$ min). *C*, PACAP38 modulation of NMDA peak currents was dose dependent. Change from baseline: control, $-1 \pm 7\%$, $n = 9$; 1 pM, $16 \pm 6\%$, $n = 4$; 10 pM, $23 \pm 5\%$, $n = 5$; 100 pM, $35 \pm 7\%$, $n = 5$; 1 nM, $44 \pm 5\%$, $n = 9$; 10 nM, $37 \pm 13\%$, $n = 6$; data obtained at 20 min of recording. *$p < 0.05$, **$p < 0.001$ versus control, ANOVA followed by *post hoc* Tukey's test. *D*, PACAP38 at 100 nM directly inhibits NMDA currents. Sample traces from the same cell are shown without 100 nM PACAP38 application (black trace) and with 100 nM PACAP38 application (gray trace) during middle 3 s of NMDA-evoked current. Inhibition by PACAP38 was measured as the percentage that the steady-state decreased. *E*, Inhibition by 100 nM PACAP was not altered by the concentration of glycine. PACAP38 at 100 nM caused equal levels of inhibition in 0.1 and 10 μM glycine (low glycine, $29 \pm 4\%$, $n = 6$; high glycine, $27 \pm 4\%$, $n = 6$; $p > 0.3$, unpaired t test). *F*, NMDA currents were only inhibited by 100 nM PACAP38. With doses from 1 pM to 100 nM, only 100 nM PACAP38 showed a significant inhibition of NMDA currents (ANOVA followed by *post hoc* Tukey's test, $p < 0.05$).

centrations but depression with higher concentrations (Roberto and Brunelli, 2000). A range of concentrations of PACAP38 were tested to ensure that the concentrations used reliably produced positive modulation without being close to the range of negative modulation. At all concentrations up to and including 10 nM, PACAP38 enhanced peak NMDA currents (Fig. 2C).

It has also been proposed that PACAP38 interacts directly

with NMDARs to potentiate their activity, perhaps by binding to the glycine site of the NMDAR (Liu and Madsen, 1997). We examined potential direct effects using a protocol whereby PACAP38 was applied during the simultaneous application of NMDA and glycine. Briefly, NMDA (and glycine) was applied using one barrel. Once the response reached a steady state, the barrel was shifted to one containing NMDA (glycine) and PACAP38 for a period of 3 s before returning to the barrel lacking PACAP38. Rapid effects of PACAP38 was assessed as a change in the steady-state current. No rapid effects were observed with concentrations of 1–10 nM PACAP38. However, when the concentration was increased to 100 nM, a depression of currents was observed (Fig. 2*D*,*F*). This depression recovered entirely within 10 s of the application of PACAP38 and likely reflects a direct inhibition of NMDARs. This rapid inhibition, measured as the percentage of decrease in steady-state currents compared with control, did not differ in low (0.1 μM) or high (10 μM) concentrations of glycine (Fig. 2*E*). This suggests that the inhibition displayed by PACAP38 was not related to the glycine binding site on the NMDAR. Because the 1 nM concentration of PACAP38 produced the greatest enhancement of NMDAR peak currents and had no direct inhibitory effect, this concentration was used throughout the remaining experiments.

To confirm that PACAP38 was signaling via activation of the G-protein-coupled PAC_1 receptors, we used PACAP(6–38), the most potent antagonist for PAC_1 receptors (Robberecht et al., 1992). Coapplications of PACAP(6–38) (10 nM) substantially attenuated the PACAP38 effect (Fig. 3*A*). When the antagonist was present, PACAP38 (1 nM) induced only a moderate ($113 \pm 5\%$; $n = 6$) increase in NMDA-evoked currents relative to controls ($141 \pm 8\%$; $n = 6$). Although the PAC_1 receptor was required for the PACAP38 effect, the possibility exists that signaling is not mediated via G-proteins because not all GPCR signaling requires heterotrimeric G-proteins (Hall et al., 1999). To ensure that the PACAP38 effect required signaling through G-proteins, GDP-β-S a competitive inhibitor for the GTP binding site on the α subunit, was included in the patch pipette. Inclusion of 20 μM GDP-β-S blocked the PACAP38-mediated increase in NMDA-evoked currents. Without inclusion of GDP-β-S in the patch pipette, PACAP38 (1 nM) increased NMDA-evoked currents ($41 \pm 7\%$; $n = 7$) above baseline (Fig. 3*B*). When GDP-β-S was included in the patch pipette, NMDA-evoked currents were $96 \pm 2\%$ ($n = 5$) of baseline (Fig. 3*B*). As a control, we showed

A

B

A

B
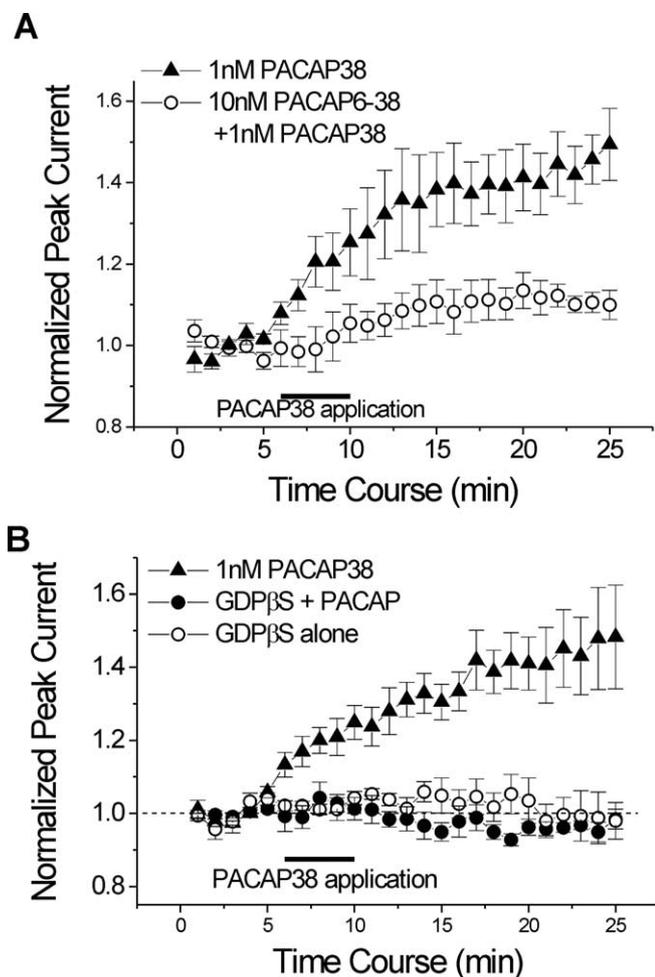
Figure 3. Effect of PACAP38 on NMDA-evoked currents requires the G-protein-coupled PAC$_1$ receptor. **A**, Addition of 10 nM PACAP(6–38), a potent antagonist of PACAP38 specific for the PAC$_1$ receptor, in all extracellular solutions for the duration of the experiment significantly attenuated the increase in NMDA-evoked currents by 1 nM PACAP38 (1 nM PACAP38, 141 ± 8%, $n = 6$; 10 nM PACAP(6–38) plus 1 nM PACAP38, 113 ± 5%, $n = 7$; $p < 0.05$, unpaired t test; data obtained at 20 min of recording). The black bar indicates time and duration of 1 nM PACAP38 application. **B**, Increased NMDA-evoked peak currents are blocked by GDP-β-S. Intracellular application of 20 μM GDP-β-S blocked the increase in NMDA-evoked peak currents by 1 nM PACAP38 (1 nM PACAP38, 141 ± 7%, $n = 7$; 1 nM PACAP38 plus 20 μM GDP-β-S, 96 ± 2%, $n = 6$; 20 μM, $p < 0.001$, unpaired t test; data obtained at 20 min of recording). Comparatively, GDP-β-S alone had no effect on NMDA-evoked currents (103 ± 6% of baseline; $n = 5$). The black bar indicates time and duration of 1 nM PACAP38 application.

Figure 4. PLCβ1 is required for the PACAP38 response. **A**, PACAP38 (1 nM) failed to elicit a response in PLCβ1 knock-out mice but produced a robust increase in NMDA-evoked peak currents in wild-type mice (wild-type mice, 144 ± 8%, $n = 10$; knock-out mice, 110 ± 5%, $n = 14$; $p < 0.001$, unpaired t test; data obtained at 20 min of recording). The black bar indicates time and duration of 1 nM PACAP38 application. **B**, Adenylyl cyclase activity was unchanged in PLCβ1 knock-out mice. Hippocampal tissue was extracted from wild-type or PLCβ1 knock-out mice, and tissue from three to five mice were pooled. Forskolin (30 μM) induced a similar fold increase in both wild-type (6.0 ± 1.3-fold increase; $n = 4$) and knock-out (4.2 ± 0.7-fold increase, $n = 4$; $p > 0.05$, unpaired t test) animals. Compared with vehicle-treated tissue, PACAP38-treated hippocampal tissue from wild-type mice had a 1.8 ± 0.3-fold ($n = 4$) increase in AC activity. In hippocampal tissue from PLCβ knock-out mice, PACAP induced a similar fold increase in AC activity (1.5 ± 0.1-fold increase, $n = 4$; $p > 0.05$, unpaired t test).

that GDP-β-S itself had no effect on NMDA-evoked currents (Fig. 3B). Because PAC$_1$Rs can signal through G$\alpha_{q/11}$ G-proteins to PLC (Zhou et al., 2001) and because PLC-mediated pathways are involved in the modulation of NMDA currents (Skeberdis et al., 2001), we decided to examine the role of PLC in the potentiation of NMDA-evoked currents by PACAP38.

For this reason, we examined CA1 neurons from PLCβ1 knock-out mice (Kim et al., 1997). In PLCβ1 knock-out mice, the effect of PACAP38 (1 nM) was markedly attenuated (110 ± 5%; $n = 14$) compared with the effect in wild-type mice (144 ± 8%; $n = 10$) (Fig. 4A). Adenylyl cyclase (AC) activity assays were performed to control for the possibility that the reduced PACAP38 response was caused by a defect in the PAC1 receptor or in AC activity in the PLCβ1 knock-out mice (Fig. 4B). Compared with vehicle-treated tissue, PACAP38-treated hippocampal tissue from wild-type mice had a 1.8 ± 0.3-fold ($n = 4$) increase in AC activity. In tissue from PLCβ1 knock-out mice,

PACAP induced a similar fold increase in AC activity (1.5 ± 0.1-fold increase; $n = 4$). The PKA activator forskolin (30 μM) also induced a similar fold increase in both wild-type (6.0 ± 1.3 fold increase; $n = 4$) and knock-out (4.2 ± 0.7-fold increase; $n = 4$; $p > 0.05$) animals (Fig. 4B). A decrease in PACAP38 modulation in PLCβ1 knock-out mice, despite PACAP38 inducing the same level of AC activation as in wild-type mice, indicates that modulation by PACAP38 is predominantly mediated through PLCβ1 and not the activation of AC. The prototypical Gα_q signaling pathway activates PLCβ and leads to the formation of inositol trisphosphate (IP$_3$) and diacylglycerol (DAG) (Neves et al., 2002). IP$_3$ formation triggers Ca^{2+} release from internal stores, which along with DAG, is required for activation of the conventional PKC isoforms (PKCα, PKCβI, PKCβII, and PKCγ) (Liu and Heckman, 1998). As such, we examined the role of calcium and PKC in mediating the PACAP38 effect.

Our patch pipette solution contains 11 mM EGTA, a Ca^{2+} chelator with slow binding kinetics. As such, inclusion of 11 mM
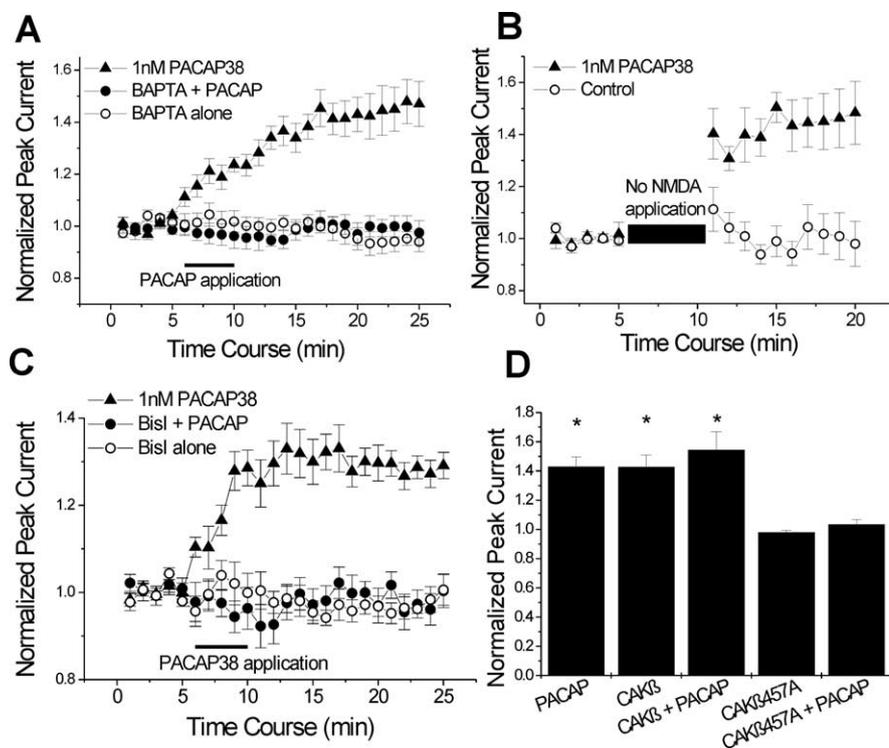
Figure 5. Intracellular calcium and calcium-activated kinases are required for the PACAP38 response. **A**, Intracellular administration of BAPTA (20 mм) blocked the PACAP38 effect and was similar to BAPTA alone (BAPTA plus PACAP38, 97 ± 4%, $n = 6$; BAPTA alone, 95 ± 4%, $n = 6$; $p > 0.2$, unpaired t test; data obtained at 20 min of recording; 1 nм PACAP38, 143 ± 7%, $n = 6$). The black bar indicates time and duration of 1 nм PACAP38 application. **B**, Blocking the entry of external calcium did not prevent PACAP-mediated enhancement of NMDA peak currents. To block external calcium entry, no NMDA was applied during the application of 1 nм PACAP38 (control, 98 ± 9%, $n = 6$; 1 nм PACAP38, 148 ± 12%, $n = 5$; $p < 0.01$, unpaired t test; data obtained at 20 min of recording). **C**, Protein kinase C is required for the PACAP38 response. Application of the PKC inhibitor bisindolylmaleimide I (500 nм) applied through internal and external solution blocked the effect of PACAP38 on NMDA-evoked currents and had no effect by itself (1 nм PACAP38, 130 ± 4%, $n = 8$; PACAP38 plus bisindolylmaleimide I, 103 ± 5%, $n = 12$; $p < 0.005$, unpaired t test; bisindolylmaleimide I alone, 97 ± 2%, $n = 5$). The black bar indicates time and duration of 1 nм PACAP38 application. **D**, Pyk2/CAKβ is required for the PACAP38 response. Intracellular application of wild-type CAKβ (0.5 μg/ml) caused an increase in NMDA-evoked peak currents, reaching a plateau after 7 min. Five minute application of PACAP38 (1 nм) on top of the plateau caused no significant increase (CAKβ before PACAP38, 142 ± 8%, $n = 6$; 5 min after PACAP38 application, 154 ± 12%, $n = 6$; $p > 0.3$, paired t test; data obtained at 10 and 25 min of recording). The PACAP38 response could be blocked by a kinase inactive mutant version of the enzyme (lysine 457 to alanine). Intracellular application of CAKβ 457A (0.5 μg/ml) blocked the effect of PACAP38 (1 nм) and was similar to CAKβ 457A applied by itself (CAKβ 457A plus 1 nм PACAP38, 103 ± 3%, $n = 6$; CAKβ alone, 98 ± 2%, $n = 5$; data obtained at 20 min of recording; *$p < 0.01$ vs CAKβ 457A and CAKβ 457A plus 1 nм PACAP38, ANOVA followed by *post hoc* Tukey's test).

EGTA in the patch pipette could potentially reduce the Ca^{2+} signal induced by PACAP application. However, in these conditions, a robust response by PACAP was seen, suggesting that, if Ca^{2+} is required for this response, EGTA is not completely blocking Ca^{2+} signaling. The amplification of the unbuffered Ca^{2+} signal by downstream signaling molecules likely overcomes any reduction in the Ca^{2+} signal by EGTA. Thus, to test whether the modulation of NMDA-evoked currents by PACAP38 required the elevation of internal Ca^{2+}, we used high concentrations of the fast Ca^{2+} chelator BAPTA (20 mм) in the patch pipette, which provides a more complete chelation of Ca^{2+} compared with EGTA. Intracellular application of 20 mм BAPTA blocked the effect of 1 nм PACAP38 (Fig. 5*A*). The application of BAPTA by itself caused no change in normalized peak NMDA currents over time. Calcium is an important signaling divalent cation that can act on many different Ca^{2+}-activated enzymes and proteins. In the case of mGluR5 potentiation of NMDARs, there is a requirement for coincident activation of NMDARs and mGluRs; without coincident activation, depression of NMDA currents occurs

(Kotecha et al., 2003). To determine whether coincident activation of NMDARs and PAC₁Rs was required in PACAP-induced signaling, NMDA was not applied during the application of PACAP38. In the absence of coincident NMDAR activation, PACAP38 was still able to potentiate NMDA-evoked currents (Fig. 5*B*). These observations indicated that coincident activation of NMDARs and PAC₁Rs is not required for PACAP potentiation of NMDA currents.

To determine the role of PKC in the PACAP38 effect, we used the PKC inhibitor bisindolylmaleimide I (bis), which has affinity for PKCα, PKCβ₁, PKCβ₁₁, PKCγ, PKCδ, and PKCε isozymes. Applications of bis (500 nм) blocked the effect of PACAP38 (97 ± 4%; $n = 6$) but had no effect when applied alone (Fig. 5*C*). These results demonstrate that the PLCβ1/PKC pathway is required for the PACAP38 modulation of NMDA-evoked currents and that the signaling pathway requires a rise in intracellular Ca^{2+}. Protein kinase C can also activate proline-rich tyrosine kinase 2, also called cell adhesion kinase β (Pyk2/CAKβ), which binds, activates, and phosphorylates Src, leading to enhanced NMDAR activity (Huang et al., 2001; Kotecha and MacDonald, 2003). Because PKC appeared to be involved in the PACAP38 effect, we tested the possibility that CAKβ is also required. Intracellular application of the functional dominant-negative mutant of CAKβ (kinase mutant, CAKβ-K457A, 0.5 μg/ml) exerted no effect on its own but blocked the PACAP38-induced potentiation of NMDA-evoked currents (Fig. 5*D*). In addition, inclusion of recombinant CAKβ (0.5 μg/ml) in the patch pipette caused a potentiation of these currents that subsequently occluded the effect of PACAP38 (Fig. 5*D*).

G-protein-coupled receptors can recruit PKC signaling pathways that activate the nonreceptor tyrosine kinases CAKβ (Dikic et al., 1996; Lu et al., 1999). Furthermore, once CAKβ is activated, the kinase autophosphorylates, creating an Src homology 2 (SH2) ligand that binds to the SH2 domain of Src, resulting in its activation (Dikic et al., 1996). As such, we looked at the role Src may have in the PACAP38-mediated increase in NMDA-evoked currents. Application of 30 U/ml recombinant Src(p60[c-src]) caused a rapid increase in normalized NMDA-evoked peak currents (Fig. 6*A*). The effect reached a plateau at 10 min, with a 46 ± 10% ($n = 6$) increase above baseline. Applications of PACAP38 (1 nм) at this point failed to elicit an additional increase, with NMDA-evoked currents measured as a 53 ± 8% ($n = 6$) increase above baseline 10 min after PACAP38 application. Intracellular application of the Src inhibitory peptide Src(40–58) completely blocked the effect of PACAP38 (Fig. 6*B*). By itself, Src(40–58) had no effect on the amplitude of NMDA-evoked currents. Block of the PACAP38 effect by the Src inhibitor and occlusion by Src(p60[c-src]) support the involvement of Src in the PACAP38-

mediated effect on NMDA-evoked currents. To further substantiate the involvement of Src, phosphorylation levels of Src were measured. Because phosphorylation of tyrosine 416 is required for activation of the kinase (Smart et al., 1981), increased phosphorylation can be used as a measure of its kinase activity. CA1 hippocampal tissue was microdissected and treated with PACAP38 or vehicle for 10 min at room temperature. Tissue was homogenized, and Src was immunoprecipitated with an antibody directed at the unique domain of Src. Subsequently blots were probed with an anti-phospho-tyrosine antibody. Phosphorylation levels were normalized to total Src. Treatment with PACAP38 increased Src phosphorylation in the CA1 region, as shown in the representative blot (Fig. 6C). The normalized density of the Src blots was measured for three such experiments and compared with control-treated tissue. A 32 ± 11% ($n = 3$) increase in phosphorylation levels was seen (Fig. 6D). Src can be tyrosine phosphorylated on many sites, including tyrosine 416, which is required for activation, and tyrosine 527, which causes inactivation of the kinase (Smart et al., 1981). To confirm that the increased tyrosine phosphorylation was activating Src, a second set of experiments was performed using site-specific antibodies for tyrosine 416 and 527. An increase of 51% was seen at Y416, although no change in phosphorylation of Y527 was observed after treatment with PACAP38. These results confirm the results seen in experiments with hippocampal slices.

To confirm that PACAP38 induces an Src-dependent potentiation of synaptic currents, we also examined spontaneous mEPSCs recorded in cultured mouse hippocampal neurons. Miniature EPSC$_{NMDA}$s were recorded for 5 min in both the absence and presence of APV (10 μM) before and after a 10 min application of PACAP38. PACAP enhanced the NMDAR component of mEPSCs by 45 ± 16% ($n = 6$) (Fig. 6E). Comparatively, the AMPA component of mEPSCs was unchanged by PACAP treatment (Fig. 6E). Inclusion of the selective Src kinase peptide inhibitor Src(40–58) in the patch pipette completely blocked the modulatory effect of PACAP38 (fractional change, 2 ± 13%; $n = 6$) (Fig. 6E). Representative mEPSCs are shown for control, APV treated (i.e., AMPA component), and after PACAP38 application (Fig. 6F).

The tyrosine kinase Fyn has also been implicated in the enhancement of NMDARs by PACAP38 (Yaka et al., 2003). This signaling pathway is believed to involve the release of Fyn kinase from the scaffolding protein RACK1. During release from RACK1, Fyn then phosphorylates the NR2B subunit, thus potentially increasing NMDAR activity (Yaka et al., 2003). In addition
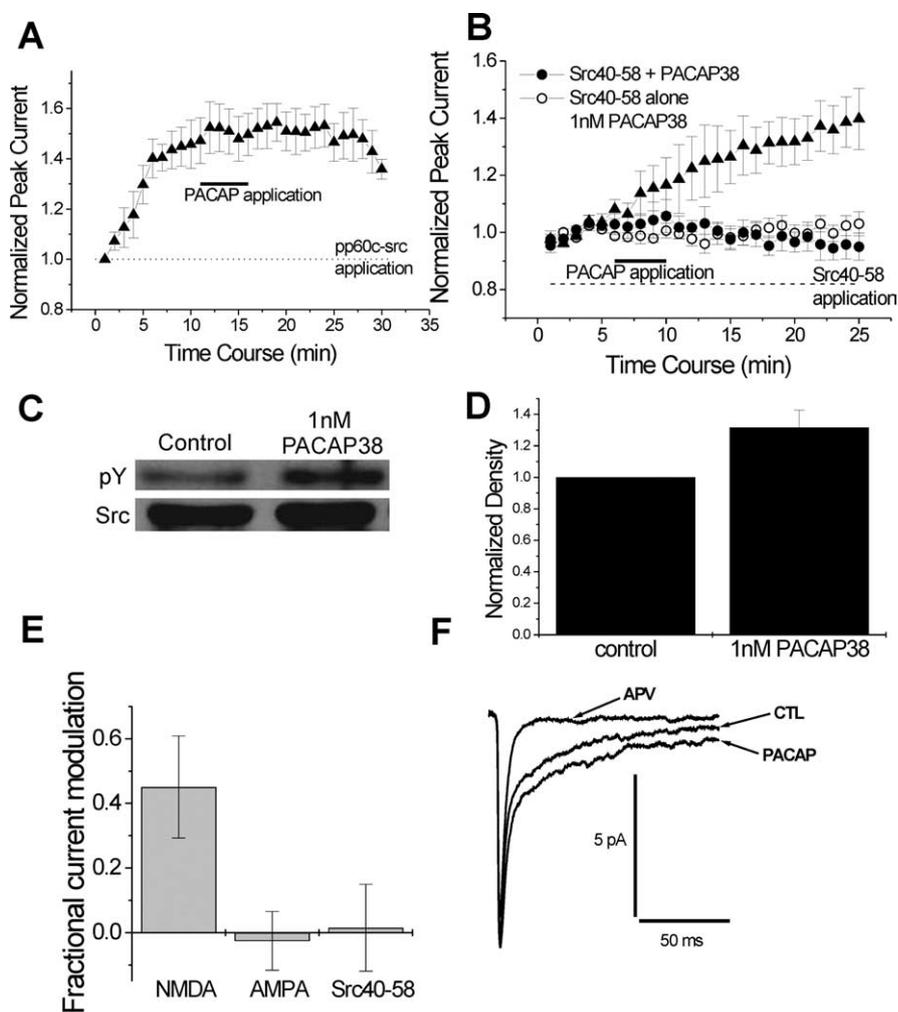
Figure 6. Nonreceptor tyrosine kinase Src is required for PACAP38 modulation of NMDA currents. *A*, Inclusion of 30 U/ml p60^{c-src} in the intracellular solution caused a rapid and sustained increase in NMDA-evoked currents that occluded the effect of 1 nM PACAP38 (before PACAP38 application, 146 ± 10%, $n = 6$; 10 min after PACAP38 application, 153 ± 8%, $n = 6$; $p > 0.5$, paired t test; data obtained at 10 and 25 min of time recording). The black bar indicates time and duration of 1 nM PACAP38 application. *B*, Inclusion of the selective Src kinase peptide inhibitor Src(40–58) at 25 μg/ml in the patch pipette completely blocked the PACAP38 response (1 nM PACAP38, 132 ± 8%, $n = 6$; Src(40–58) plus 1 nM PACAP38, 100 ± 3%, $n = 8$; $p < 0.005$, unpaired t test; data obtained at 20 min of recording). Inclusion of Src(40–58) by itself had no effect [Src(40–58) alone, 97 ± 4%, $n = 6$; data obtained at 20 min of recording]. *C, D*, Activation of Src by 1 nM PACAP38 was determined by phosphorylation levels of Src. Microdissected CA1 hippocampal tissue was treated with vehicle or 1 nM PACAP38 for 10 min. Src was immunoprecipitated and probed with a phosphotyrosine antibody. Phosphorylation levels were normalized to the total amount of Src loaded and measured as a relative change compared with control. PACAP38 treatment increased tyrosine phosphorylation levels 32 ± 11% ($n = 3$) above vehicle-treated tissue. *E*, PACAP38 increased the NMDA component of mEPSPs, and the increase was Src dependent. Application of PACAP38 (1 nM) to cultured hippocampal neurons for 5 min increased the NMDA component of miniature EPSPs by 45 ± 16% ($n = 6$). Comparatively, the AMPA component of the mEPSPs was unchanged, with a fractional current modulation of −3 ± 9% ($n = 6$). Inclusion of the selective Src kinase peptide inhibitor Src(40–58) at 25 μg/ml in the patch pipette completely blocked the PACAP38 response (fractional change, 1.5 ± 13%; $n = 5$). *F*, Sample traces are shown for control, APV treated (i.e., AMPA component), and after PACAP38 treatment.

to Fyn, RACK1 binds various signaling intermediates, including but not limited to PKCβII (Ron and Mochly-Rosen, 1994), PLCγ (Disatnik et al., 1994), and Src (Chang et al., 1998). Sequestering of Fyn and Src kinases by RACK1 blocked the ability of these kinases to participate in cell signaling (Chang et al., 1998; Yaka et al., 2002). The reported Fyn binding site on RACK1 is located in tryptophan-aspartate (WD) repeat 1 and includes amino acids 35–48 (Yaka et al., 2002). Comparatively, the Src binding site on RACK1 is located in WD repeat 6, with phosphorylated tyrosines at positions 228 and 246 playing key roles in the degree of binding of Src (Chang et al., 2001). In the case of Fyn, introduction of a
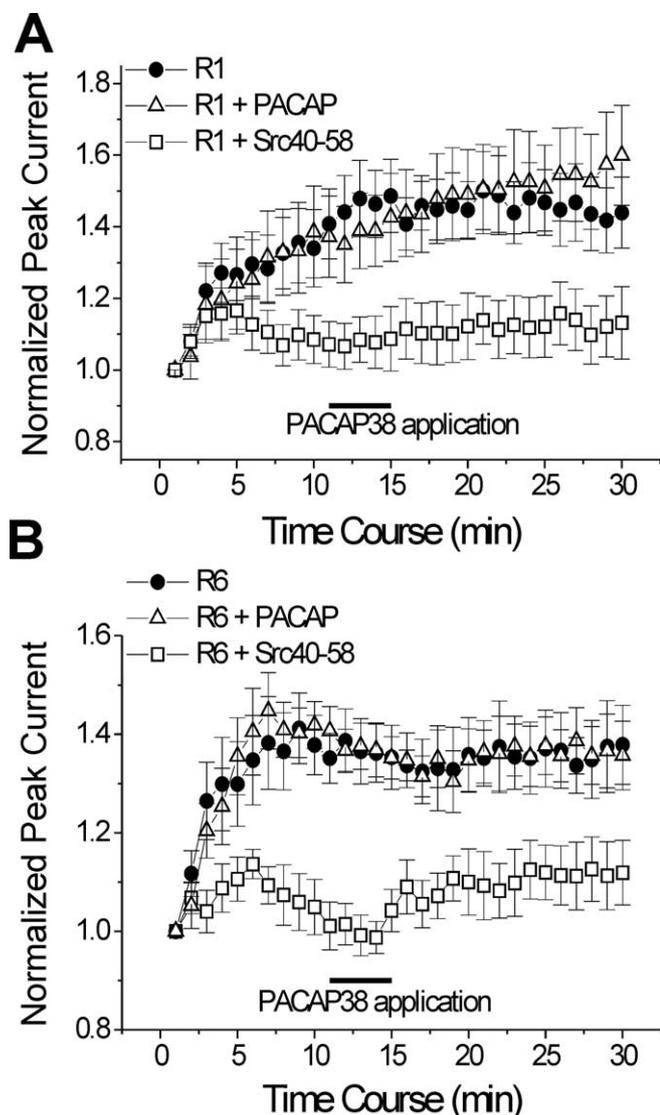
Figure 7. Binding of Src to the scaffolding protein RACK1 is required for PACAP modulation. *A*, Inclusion of 100 μM R1 in the patch pipette caused an increase in normalized NMDA peak currents. In a separate group of cells, the external application of 1 nM PACAP38 caused no additional enhancement of NMDA peak currents. When the selective Src kinase peptide inhibitor Src(40–58) at 25 μg/ml was included in the patch along with 100 μM R1, the potentiation of peak currents was severely attenuated: R1 alone, 147 ± 9%, $n = 7$; R1 plus PACAP38, 150 ± 12%, $n = 7$; R1 plus Src(40–58), 112 ± 9%, $n = 9$; data obtained at 25 min of recording. *$p < 0.05$ versus R1 plus Src(40–58), ANOVA followed by *post hoc* Tukey's test. The black bar indicates application of PACAP38. *B*, Inclusion of 100 μM R6 resulted in a similar pattern as that for experiments with the R1 peptide: R6 alone, 137 ± 8%, $n = 7$; R6 plus PACAP38, 138 ± 6%, $n = 6$; R6 plus Src(40–58), 112 ± 6%, $n = 6$; data obtained at 25 min of recording. *$p < 0.05$ versus R6 plus Src(40–58), ANOVA followed by *post hoc* Tukey's test. The black bar indicates application of PACAP38.

small peptide corresponding to the Fyn binding site in RACK1 disrupts the binding of RACK1 and Fyn and increases the ability of the kinase to signal (Yaka et al., 2002). Therefore, to test the involvement of the scaffolding protein RACK1 in mediating the signaling pathway by PACAP, we synthesized two peptides, one corresponding to the Fyn binding site in WD repeat 1 (Yaka et al., 2002) and one corresponding to the Src binding site in WD repeat 6 (Chang et al., 2001), which we named R1 and R6, respectively. Inclusion of either peptide in the patch pipette at a concentration of 100 μM caused an increase in evoked NMDA peak currents (Fig. 7*A*,*B*). The increase induced by inclusion of R1 was slower

and larger than the increase induced by inclusion of R6. In both cases, when PACAP38 was applied after the induction of potentiation, no additional increase was observed. This suggests that RACK1 is required for enhancement of NMDAR currents by PACAP38. However, these results introduce the conundrum that the signaling could be either Fyn or Src mediated. To resolve this issue, we used the Src-specific inhibitory peptide Src(40–58), which was applied through the patch pipette along with either R1 or R6. In both cases, inclusion of 25 μg/ml Src(40–58) blocked the ability of the RACK1 peptides to induce an increase in NMDA peak currents. This implies that for both circumstances Src is mediating the ability of PACAP38 to modulate NMDAR activity.

Discussion

The mechanism whereby PACAP modulates NMDARs is poorly understood but is of great interest because these receptors are essential in development, synaptic plasticity, and excitotoxicity (McBain and Mayer, 1994; Dingledine et al., 1999). Here we have shown that PACAP38 increases Schaffer collateral EPSC$_{NMDA}$s, miniature EPSC$_{NMDA}$s in cultured hippocampal neurons, and peak NMDAR currents in isolated CA1 hippocampal neurons. All of these responses to PACAP38 were blocked when the Src inhibitor peptide was included in the patch electrode. Furthermore, the response in isolated neurons was blocked by the antagonist PACAP(6–38), confirming that this signal was mediated by the PAC$_1$ receptor. Additionally, signaling through heterotrimeric G-proteins was confirmed using GDP-β-S, a competitive inhibitor for the GTP binding site. The large reduction in the response to PACAP seen in CA1 neurons taken from PLCβ1 knock-out mice, without any change in the production of cAMP, strongly suggests that PACAP enhances NMDARs via Gα_q and not Gα_s. A major role for PKC signaling in this pathway is further implicated because bisindolylmaleimide I, an inhibitor of PKC, blocks the PACAP38 effect.

PKC enhances NMDARs in CA1 neurons through the activation of the nonreceptor tyrosine kinases CAKβ (Pyk2) and Src (Lu et al., 1999; Huang et al., 2001; Benquet et al., 2002; Gerber, 2002; Alier and Morris, 2005; Grishin et al., 2005). Here we have shown that applications of recombinant CAKβ or Src induce an increase of NMDAR peak currents that occlude the effect of PACAP38. PACAP38 also increased phosphorylation of endogenous Src at tyrosine 416 indicative of kinase activation. A functionally dominant-negative form of recombinant CAKβ, CAKβ 457A, and the Src specific inhibitor Src(40–58) both blocked the potentiation of NMDA currents by PACAP38. Therefore, our results are consistent with PAC$_1$R activation enhancing NMDAR activity via stimulation of the sequential signaling by PKC/CAKβ/Src.

Our results are in accordance with previous studies in which PACAP38 enhanced NMDAR activity in the hippocampal CA1 region (Wu and Dun, 1997; Roberto and Brunelli, 2000; Yaka et al., 2003). However, Liu and Madsen (1997) proposed that PACAP38 modulates NMDARs by a direct effect of PACAP38 on the NMDAR, possibly acting through the glycine binding site. Contrary to this finding, we have shown that low concentrations of PACAP38 act through the PAC$_1$ receptor to enhance NMDA currents. PACAP38 at high concentrations (100 nM) may directly inhibit NMDARs, although we found no dependency on the concentrations of glycine suggesting that this is not via an interaction with the glycine binding site.

PACAP has been reported to cause the release of neurotrophic factors from astrocytes (Pellegri et al., 1998). Release of neurotrophic factors, such as BDNF, likely contributes to the neuro-

protective effects of PACAP, but these factors may also act as regulators of NMDAR activity themselves (Jarvis et al., 1997). Furthermore, Roberto and Brunelli (2000) suggest that PACAP may mediate its effects presynaptically by altering muscarinic activity. However, the use of isolated CA1 neurons as well as intracellular applications of agents via the patch pipette have allowed us to determine the major signal components responsible for the postsynaptic regulation of NMDARs by PAC$_1$Rs.

Previously, a role for Fyn, a related Src family kinase, was proposed in PACAP38 signaling (Yaka et al., 2003). In this proposed model, Fyn is inhibited by its binding to RACK1, and PKA stimulates translocation of RACK1 to the nucleus, freeing Fyn to phosphorylate NMDARs (Yaka et al., 2002, 2003). However, Src also binds to RACK1 (Chang et al., 1998, 2001), and RACK1 reduces of the activity of both tyrosine kinases (Chang et al., 1998; Yaka et al., 2002). In isolated CA1 neurons, introduction of peptides homologous either to the binding site on RACK1 for Fyn (R1) or Src (R6) increased peak NMDA currents presumably by disinhibiting these kinases. Applications of PACAP38 on top of this enhancement had no additional effect, suggesting that the disruption of this binding disrupts the signaling induced by PACAP38. To ensure that it was the release of Src that was mediating the response to the peptides, the Src inhibitory peptide Src(40–58) was included in the patch pipette along with the RACK1 peptides. Inclusion of the Src-selective inhibitor abolished the increase of current seen when R1 or R6 was applied to the cells. The inhibitor peptide Src(40–58) mimics the unique region of Src and not regions of any of the other Src family tyrosine kinases. Most importantly, Src binds by its unique domain to an identified region of ND2, a protein that serves as the major scaffolding protein for Src at hippocampal synapses (Gingrich et al., 2004). Other Src kinases, including Fyn, do not. Indeed, Src(40–58) acts by displacing Src from ND2, and this inhibitor does not alter the association of ND2 with NMDARs, nor does it alter the catalytic activity of Src (Gingrich et al., 2004). Our results suggest that the actions of Fyn kinase on NMDARs depends on the subsequent activation of Src. Therefore, as RACK1 binds activated PKC, Fyn, and Src, it may act as a hub (Ron and Mochly-Rosen, 1994; Chang et al., 1998) in which CAKβ can be activated by PKC in the correct spatial arrangement to activate Src.

This study contributes to the growing body of evidence demonstrating a role for PACAP modulation of NMDAR activity. Indeed, many physiological roles attributed to NMDA are also attributed to PACAP. One role for NMDARs is development (Arimura et al., 1994; Jaworski and Proctor, 2000). Similarly, PACAP expression also has an essential role in development, and this is most clearly seen in PACAP$^{-/-}$ animals, which display high mortality rates soon after birth (Hashimoto et al., 2000; Sauvage et al., 2000; Gray et al., 2001). Furthermore, both PACAP and NMDARs play a role in learning and memory. In the CA1 region of the hippocampus, increased NMDAR activity and increased Ca^{2+} entry through the receptor is required for the formation of LTP (Collingridge and Bliss, 1995). It is believed that LTP represents the cellular basis for learning and memory. Because PACAP38 can increase NMDAR activity, it is not surprising that PACAP and its signaling pathways have been linked to learning and memory. In experiments using hippocampal slices, PACAP38 has been shown to increase field EPSPs (Roberto and Brunelli, 2000; Yaka et al., 2003). This change in synaptic strength by PACAP38 is thought to contribute to the long-term changes associated with learning and memory. Indeed, this paper shows that PACAP38 can increase the amplitude of NMDA currents in hippocampal slice. A role for PACAP in learning and memory

clearly exists, but experimental results suggest that this role may be complex. Experiments with PAC$_1$R$^{-/-}$ mice have shown learning deficits in traditional hippocampal-dependent tasks, such as associative memory tasks, whereas hippocampal-dependent declarative memory tests, such as the Morris water maze, are unaffected (Sauvage et al., 2000; Otto et al., 2001). The lack of effect in declarative learning might be explained by VPAC$_1$ and VPAC$_2$ receptors compensating for the lack of PAC$_1$Rs. Use of PACAP$^{-/-}$ mice in learning paradigms would assist in clarifying the role of PACAP in learning and memory. However, as mentioned previously, PACAP$^{-/-}$ mice display high mortality rates (Hashimoto et al., 2000; Sauvage et al., 2000; Gray et al., 2001). PACAP$^{-/-}$ mice also display aberrations to psychomotor behavior, including increased ambulation, explosive jumping, decreased anxiety, and altered mating behavior, which can be relieved with antipsychotics (Hashimoto et al., 2001). Interestingly, transgenic mice that express only a small percentage of the NR1 subunit exhibit many similar behaviors, also relieved by the typical antipsychotic haloperidol and the atypical antipsychotic clozapine (Mohn et al., 1999). These NR1 transgenic mice provide evidence for the hypoglutamatergic model of schizophrenia in which decreased glutamate activity, especially decreased NMDAR activity, contributes to schizophrenic symptoms (Morris et al., 2005). This hypothesis is supported by evidence that administration of the NMDAR antagonist phencyclidine to humans causes both positive and negative symptoms associated with schizophrenia (Morris et al., 2005). Similarities between these two animal knock-outs suggest that deficits in PACAP and the PACAP receptor systems could contribute to the symptoms associated with schizophrenia. This forms an interesting but as of yet untested hypothesis.

In summary, we have shown that PACAP38 mediates an increase of NMDA currents via a PKC signaling pathway. Intermediates of this pathway include PLCβ1, Ca^{2+}, CAKβ, and Src. Furthermore, the scaffolding protein RACK1 is required for this pathway, by binding Src. This pathway does not require PKA and as such represents a novel pathway for the mediation of PACAP38-induced changes in NMDA activity. The link between PACAP and NMDAR systems is strengthened by our results suggesting that PACAP may be involved in many of the physiological roles attributed to NMDARs.

References

Alier KA, Morris BJ (2005) Divergent regulation of Pyk2/CAKbeta phosphorylation by Ca^{2+} and cAMP in the hippocampus. Biochim Biophys Acta

Arimura A, Somogyvari-Vigh A, Weill C, Fiore RC, Tatsuno I, Bay V, Brenneman DE (1994) PACAP functions as a neurotrophic factor. Ann NY Acad Sci 739:228–243.

Benquet P, Gee CE, Gerber U (2002) Two distinct signaling pathways upregulate NMDA receptor responses via two distinct metabotropic glutamate receptor subtypes. J Neurosci 22:9679–9686.

Chang BY, Conroy KB, Machleder EM, Cartwright CA (1998) RACK1, a receptor for activated C kinase and a homolog of the beta subunit of G proteins, inhibits activity of src tyrosine kinases and growth of NIH 3T3 cells. Mol Cell Biol 18:3245–3256.

Chang BY, Chiang M, Cartwright CA (2001) The interaction of Src and RACK1 is enhanced by activation of protein kinase C and tyrosine phosphorylation of RACK1. J Biol Chem 276:20346–20356.

Collingridge GL, Bliss TV (1995) Memories of NMDA receptors and LTP. Trends Neurosci 18:54–56.

Conn PJ (2003) Physiological roles and therapeutic potential of metabotropic glutamate receptors. Ann NY Acad Sci 1003:12–21.

Dikic I, Tokiwa G, Lev S, Courtneidge SA, Schlessinger J (1996) A role for Pyk2 and Src in linking G-protein-coupled receptors with MAP kinase activation. Nature 383:547–550.

Dingledine R, Borges K, Bowie D, Traynelis SF (1999) The glutamate receptor ion channels. Pharmacol Rev 51:7–61.

Disatnik MH, Hernandez-Sotomayor SM, Jones G, Carpenter G, Mochly-Rosen D (1994) Phospholipase C-gamma 1 binding to intracellular receptors for activated protein kinase C. Proc Natl Acad Sci USA 91:559–563.

Gerber U (2002) G-protein-coupled receptors, tyrosine kinases and neurotransmission. Neuropharmacology 42:587–592.

Gingrich JR, Pelkey KA, Fam SR, Huang YQ, Petralia RS, Wenthold RJ, Salter MW (2004) Unique domain anchoring of Src to synaptic NMDA receptors via the mitochondrial protein NADH dehydrogenase subunit 2. Proc Natl Acad Sci USA 101:6237–6242.

Gray SL, Cummings KJ, Jirik FR, Sherwood NM (2001) Targeted disruption of the pituitary adenylate cyclase-activating polypeptide gene results in early postnatal death associated with dysfunction of lipid and carbohydrate metabolism. Mol Endocrinol 15:1739–1747.

Grishin AA, Benquet P, Gerber U (2005) Muscarinic receptor stimulation reduces NMDA responses in CA3 hippocampal pyramidal cells via Ca^{2+}-dependent activation of tyrosine phosphatase. Neuropharmacology 49:328–337.

Hall RA, Premont RT, Lefkowitz RJ (1999) Heptahelical receptor signaling: beyond the G protein paradigm. J Cell Biol 145:927–932.

Harrison PJ, Weinberger DR (2005) Schizophrenia genes, gene expression, and neuropathology: on the matter of their convergence. Mol Psychiatry 10:40–68.

Hashimoto H, Ishihara T, Shigemoto R, Mori K, Nagata S (1993) Molecular cloning and tissue distribution of a receptor for pituitary adenylate cyclase-activating polypeptide. Neuron 11:333–342.

Hashimoto H, Shintani N, Nishino A, Okabe M, Ikawa M, Matsuyama S, Itoh K, Yamamoto K, Tomimoto S, Fujita T, Hagihara N, Mori W, Koyama Y, Matsuda T, Nagata S, Baba A (2000) Mice with markedly reduced PACAP (PAC(1)) receptor expression by targeted deletion of the signal peptide. J Neurochem 75:1810–1817.

Hashimoto H, Shintani N, Tanaka K, Mori W, Hirose M, Matsuda T, Sakaue M, Miyazaki J, Niwa H, Tashiro F, Yamamoto K, Koga K, Tomimoto S, Kunugi A, Suetake S, Baba A (2001) Altered psychomotor behaviors in mice lacking pituitary adenylate cyclase-activating polypeptide (PACAP). Proc Natl Acad Sci USA 98:13355–13360.

Hashimoto H, Shintani N, Baba A (2002) Higher brain functions of PACAP and a homologous Drosophila memory gene amnesiac: insights from knockouts and mutants. Biochem Biophys Res Commun 297:427–431.

Huang Y, Lu W, Ali DW, Pelkey KA, Pitcher GM, Lu YM, Aoto H, Roder JC, Sasaki T, Salter MW, MacDonald JF (2001) CAKbeta/Pyk2 kinase is a signaling link for induction of long-term potentiation in CA1 hippocampus. Neuron 29:485–496.

Jarvis CR, Xiong Z, Plant JR, Churchill D, Lu W, MacVicar BA, MacDonald JF (1997) Neurotrophin modulation of NMDA receptors in cultured murine and isolated rat neurons. J Neurophysiol 78:2363–2371.

Jaworski DM, Proctor MD (2000) Developmental regulation of pituitary adenylate cyclase-activating polypeptide and PAC(1) receptor mRNA expression in the rat central nervous system. Brain Res Dev Brain Res 120:27–39.

Kim D, Jun KS, Lee SB, Kang NG, Min DS, Kim YH, Ryu SH, Suh PG, Shin HS (1997) Phospholipase C isozymes selectively couple to specific neurotransmitter receptors. Nature 389:290–293.

Kotecha SA, MacDonald JF (2003) Signaling molecules and receptor transduction cascades that regulate NMDA receptor-mediated synaptic transmission. Int Rev Neurobiol 54:51–106.

Kotecha SA, Jackson MF, Al Mahrouki A, Roder JC, Orser BA, MacDonald JF (2003) Co-stimulation of mGluR5 and N-methyl-D-aspartate receptors is required for potentiation of excitatory synaptic transmission in hippocampal neurons. J Biol Chem 278:27742–27749.

Liu GJ, Madsen BW (1997) PACAP38 modulates activity of NMDA receptors in cultured chick cortical neurons. J Neurophysiol 78:2231–2234.

Liu WS, Heckman CA (1998) The sevenfold way of PKC regulation. Cell Signal 10:529–542.

Lu WY, Xiong ZG, Lei S, Orser BA, Dudek E, Browning MD, MacDonald JF (1999) G-protein-coupled receptors act via protein kinase C and Src to regulate NMDA receptors. Nat Neurosci 2:331–338.

MacDonald JF, Mody I, Salter MW (1989) Regulation of N-methyl-D-aspartate receptors revealed by intracellular dialysis of murine neurones in culture. J Physiol (Lond) 414:17–34.

MacDonald JF, Kotecha SA, Lu WY, Jackson MF (2001) Convergence of PKC-dependent kinase signal cascades on NMDA receptors. Curr Drug Targets 2:299–312.

Marino MJ, Conn PJ (2002a) Direct and indirect modulation of the N-methyl-D-aspartate receptor. Curr Drug Targets CNS Neurol Disord 1:1–16.

Marino MJ, Conn JP (2002b) Modulation of the basal ganglia by metabotropic glutamate receptors: potential for novel therapeutics. Curr Drug Targets CNS Neurol Disord 1:239–250.

Matsuyama S, Matsumoto A, Hashimoto H, Shintani N, Baba A (2003) Impaired long-term potentiation in vivo in the dentate gyrus of pituitary adenylate cyclase-activating polypeptide (PACAP) or PACAP type 1 receptor-mutant mice. NeuroReport 14:2095–2098.

McBain CJ, Mayer ML (1994) N-methyl-D-aspartic acid receptor structure and function. Physiol Rev 74:723–760.

McCulloch DA, MacKenzie CJ, Johnson MS, Robertson DN, Holland PJ, Ronaldson E, Lutz EM, Mitchell R (2002) Additional signals from VPAC/PAC family receptors. Biochem Soc Trans 30:441–446.

Mohn AR, Gainetdinov RR, Caron MG, Koller BH (1999) Mice with reduced NMDA receptor expression display behaviors related to schizophrenia. Cell 98:427–436.

Morris BJ, Cochran SM, Pratt JA (2005) PCP: from pharmacology to modelling schizophrenia. Curr Opin Pharmacol 5:101–106.

Neves SR, Ram PT, Iyengar R (2002) G protein pathways. Science 296:1636–1639.

Nguyen PV, Woo NH (2003) Regulation of hippocampal synaptic plasticity by cyclic AMP-dependent protein kinases. Prog Neurobiol 71:401–437.

Ohtaki T, Masuda Y, Ishibashi Y, Kitada C, Arimura A, Fujino M (1993) Purification and characterization of the receptor for pituitary adenylate cyclase-activating polypeptide. J Biol Chem 268:26650–26657.

Otto C, Kovalchuk Y, Wolfer DP, Gass P, Martin M, Zuschratter W, Grone HJ, Kellendonk C, Tronche F, Maldonado R, Lipp HP, Konnerth A, Schutz G (2001) Impairment of mossy fiber long-term potentiation and associative learning in pituitary adenylate cyclase activating polypeptide type I receptor-deficient mice. J Neurosci 21:5520–5527.

Pellegri G, Magistretti PJ, Martin JL (1998) VIP and PACAP potentiate the action of glutamate on BDNF expression in mouse cortical neurones. Eur J Neurosci 10:272–280.

Robberecht P, Gourlet P, de Neef P, Woussen-Colle MC, Vandermeers-Piret MC, Vandermeers A, Christophe J (1992) Structural requirements for the occupancy of pituitary adenylate-cyclase-activating-peptide (PACAP) receptors and adenylate cyclase activation in human neuroblastoma NB-OK-1 cell membranes. Discovery of PACAP(6–38) as a potent antagonist. Eur J Biochem 207:239–246.

Roberto M, Brunelli M (2000) PACAP-38 enhances excitatory synaptic transmission in the rat hippocampal CA1 region. Learn Mem 7:303–311.

Ron D, Mochly-Rosen D (1994) Agonists and antagonists of protein kinase C function, derived from its binding proteins. J Biol Chem 269:21395–21398.

Sauvage M, Brabet P, Holsboer F, Bockaert J, Steckler T (2000) Mild deficits in mice lacking pituitary adenylate cyclase-activating polypeptide receptor type 1 (PAC1) performing on memory tasks. Brain Res Mol Brain Res 84:79–89.

Shintani N, Hashimoto H, Baba A (2004) Altered higher brain function in PACAP-knockout mice (in Japanese). Nippon Yakurigaku Zasshi 123:274–280.

Shioda S, Ozawa H, Dohi K, Mizushima H, Matsumoto K, Nakajo S, Takaki A, Zhou CJ, Nakai Y, Arimura A (1998) PACAP protects hippocampal neurons against apoptosis: involvement of JNK/SAPK signaling pathway. Ann NY Acad Sci 865:111–117.

Skeberdis VA, Lan J, Opitz T, Zheng X, Bennett MV, Zukin RS (2001) mGluR1-mediated potentiation of NMDA receptors involves a rise in intracellular calcium and activation of protein kinase C. Neuropharmacology 40:856–865.

Skoglosa Y, Takei N, Lindholm D (1999) Distribution of pituitary adenylate cyclase activating polypeptide mRNA in the developing rat brain. Brain Res Mol Brain Res 65:1–13.

Smart JE, Oppermann H, Czernilofsky AP, Purchio AF, Erikson RL, Bishop JM (1981) Characterization of sites for tyrosine phosphorylation in the transforming protein of Rous sarcoma virus (pp60v-src) and its normal cellular homologue (pp60c-src). Proc Natl Acad Sci USA 78:6013–6017.

Spengler D, Waeber C, Pantaloni C, Holsboer F, Bockaert J, Seeburg PH,

Journot L (1993) Differential signal transduction by five splice variants of the PACAP receptor. Nature 365:170–175.

Wang LY, MacDonald JF (1995) Modulation by magnesium of the affinity of NMDA receptors for glycine in murine hippocampal neurones. J Physiol (Lond) 486:83–95.

Wittmann M, Marino MJ, Henze DA, Seabrook GR, Conn PJ (2005) Clozapine potentiation of N-methyl-D-aspartate receptor currents in the nucleus accumbens: role of NR2B and protein kinase A/Src kinases. J Pharmacol Exp Ther 313:594–603.

Wong AH, Van Tol HH (2003) Schizophrenia: from phenomenology to neurobiology. Neurosci Biobehav Rev 27:269–306.

Wu SY, Dun NJ (1997) Potentiation of NMDA currents by pituitary adenylate cyclase activating polypeptide in neonatal rat sympathetic preganglionic neurons. J Neurophysiol 78:1175–1179.

Yaka R, Thornton C, Vagts AJ, Phamluong K, Bonci A, Ron D (2002) NMDA receptor function is regulated by the inhibitory scaffolding protein, RACK1. Proc Natl Acad Sci USA 99:5710–5715.

Yaka R, He DY, Phamluong K, Ron D (2003) Pituitary adenylate cyclase-activating polypeptide (PACAP(1–38)) enhances N-methyl-D-aspartate receptor function and brain-derived neurotrophic factor expression via RACK1. J Biol Chem 278:9630–9638.

Yamamoto K, Hashimoto H, Hagihara N, Nishino A, Fujita T, Matsuda T, Baba A (1998) Cloning and characterization of the mouse pituitary adenylate cyclase-activating polypeptide (PACAP) gene. Gene 211:63–69.

Zhou CJ, Kikuyama S, Arimura A, Shioda S (2000a) Distribution of PACAP receptor and its splice variants in the rat brain by in situ RT-PCR. Ann NY Acad Sci 921:373–374.

Zhou CJ, Kikuyama S, Nakajo S, Arimura A, Shioda S (2000b) Ontogeny of PACAP receptor and its splice variants in the rat brain. Ann NY Acad Sci 921:375–376.

Zhou CJ, Yada T, Kohno D, Kikuyama S, Suzuki R, Mizushima H, Shioda S (2001) PACAP activates PKA, PKC and Ca^{2+} signaling cascades in rat neuroepithelial cells. Peptides 22:1111–1117.